ACCSCIENCE PUBLISHING

International Journal of Bioprinting

RESEARCH ARTICLE

Design, fabrication, and evaluation of a novel 3D-printed temporomandibular joint prosthesis enhanced with elastic layers

Junqi Jiang[1], Zhiwei Jiao[2], Bingxue Cheng[3], Jianmin Han[4], Xiangliang Xu[1]*, and Chuanbin Guo[1]*

[1]Department of Oral and Maxillofacial Surgery, National Center of Stomatology and National Clinical Research Center for Oral Diseases and National Engineering Research Center of Oral Biomaterials and Digital Medical Devices and Beijing Key Laboratory of Digital Stomatology and Research Center of Engineering and Technology for Computerized Dentistry Ministry of Health and NMPA Key Laboratory for Dental Materials, Peking University School and Hospital of Stomatology, Beijing, China

[2]College of Mechanical and Electrical Engineering, Beijing University of Chemical Technology, Beijing, China

[3]State Key Laboratory of Tribology in Advanced Equipment, Tsinghua University, Beijing, China

[4]Tianjin Medical University School and Hospital of Stomatology & Tianjin Key Laboratory of Oral Soft and Hard Tissues Restoration and Regeneration Department, Tianjin, China

***Corresponding authors:**
XiangLiang Xu
(kqxxl@126.com)

Chuanbin Guo
(guodazuo@sina.com)

Citation: Jiang J, Jiao Z, Cheng B, Han J, Xu X, Guo C. Design, fabrication and evaluation of a novel 3D-printed temporomandibular joint prosthesis enhanced with elastic layers. *Int J Bioprint*. 2025;11(1):301-313. doi: 10.36922/ijb.4899

Received: September 20, 2024
1st revised: October 22, 2024
2nd revised: November 9, 2024
Accepted: November 20, 2024
Published Online: November 20, 2024

Copyright: © 2024 Author(s). This is an Open Access article distributed under the terms of the Creative Commons Attribution License, permitting distribution, and reproduction in any medium, provided the original work is properly cited.

Publisher's Note: AccScience Publishing remains neutral with regard to jurisdictional claims in published maps and institutional affiliations.

Abstract

Artificial temporomandibular joint (TMJ) replacement is a common intervention for the treatment of advanced TMJ diseases and ankylosis. The present study addresses the insufficient elasticity of existing artificial TMJs through the development of a composite material by incorporating high-density polyethylene into ultra-high-molecular-weight polyethylene. This was processed using fused deposition modeling 3D-printing technology to produce porous elastic layers with an elastic modulus similar to that of joint discs. An artificial TMJ prosthesis with physiological elasticity was successfully fabricated, applied to the surface of porous Ti–6Al–4V alloy, and validated through mechanical experiments. The results demonstrated that the elastic modulus of the synthetic cartilage exhibits a negative correlation with the number of staggered layers, while no significant relationship was observed between the elastic modulus and the alternating angle between the harnesses. The elastic modulus of the cartilage was measured to be 127.5 ± 16.1 MPa, while the maximum compressive strength was found to be 8.0 ± 1.3 MPa. Optimal performance was observed for a staggered layer count of five and a cross-angle of 90°. The bonding strength to the metal mandibular prosthesis was measured to be 2.62 ± 0.98 MPa, and the surface roughness was determined to be 1.6 μm. An elastic artificial TMJ process prosthesis in this study was successfully designed, fabricated, and validated through *in vitro* experiments, offering valuable insights for future advancements in artificial TMJ design.

Keywords: 3D printing; Artificial temporomandibular joint replacement; Elasticity; Porous elastic layers; Ultra-high-molecular-weight polyethylene; Ti–6Al–4V alloy

1. Introduction

Reconstruction of the temporomandibular joint (TMJ) typically involves autogenous bone grafting or the utilization of alloplastic TMJ implants. Compared with autogenous reconstruction, alloplastic TMJ replacement offers advantages in terms of reduced donor-site morbidity, shorter surgical duration, and the customizability to fit specific anatomical requirements.[1] Currently, the majority of TMJ prostheses consist of two components: an artificial fossa prosthesis constructed from ultra-high-molecular-weight polyethylene (UHMWPE) and an artificial condyle prosthesis composed of metal. There are two primary categories of TMJ prostheses available for clinical utilization: the stock Zimmer Biomet products and custom-made TMJ concepts products.[2] These artificial TMJ prostheses have been widely employed in clinical settings.[3] Nevertheless, it is important to note that current artificial TMJ prostheses systems do not feature biomimetic articular discs or articular cartilage structure, and this has significant implications related to their biomechanical differences from natural anatomical structures.[2] During mandibular movement, the discs exhibit a viscoelastic response to both static and dynamic loading, effectively absorbing stress.[4] Additionally, changes in loading patterns subsequent to reconstructive surgery can induce stress variations in the bilateral TMJ discs, which could potentially lead to calcification.[5] The disc functions as a vital cushioning element for the condylar prosthesis, and its absence may influence the resorption of healthy bone and the mobility of the healthy TMJ.

Elastic structures such as articular discs and cartilage are very important for the long-term functional movement of TMJs.[4,6] Accordingly, the lack of physiological elasticity during functional movement is a notable limitation of existing artificial TMJ prostheses. For instance, Xu et al.[7] compared the biomechanical behaviors of a custom-made mandibular condyle prosthesis and a total TMJ prosthesis using the finite element method. Their results showed that TMJ prosthesis materials with high Young's moduli affect the contralateral TMJ. Therefore, along with their morphology, the elasticity of TMJ prostheses should also be considered in the future.

Ti alloys and UHMWPE are commonly utilized materials in TMJ prostheses. Ti alloys are known for their high strength, low modulus of elasticity, and excellent biocompatibility. They are typically employed in the construction of the ramus of the condyle in U.S. Food and Drug Administration (FDA)-approved TMJ implants.[8] UHMWPE is a linear polyethylene with a high molecular weight that offers superior properties in terms of wear resistance, impact resistance, chemical resistance, and a low coefficient of friction.[9] This polymer is commonly used in the construction of the fossa of TMJ prostheses.

The utilization of additive manufacturing techniques has become prevalent in the fabrication of customized TMJ prostheses. Research has demonstrated the ability of selective laser melting to accurately construct the architecture of Ti alloys, while fused deposition modeling (FDM) has been employed to create objects from UHMWPE.[10,11] Thus, the application of these materials using these methods may present a novel approach to fabricating TMJ prostheses with enhanced comfort and longevity.

UHMWPE is a widely employed polymer with numerous excellent qualities. Since the 1960s, UHMWPE has been utilized in total joint replacements, including arthroplasty of the hip, knee, shoulder, and intervertebral discs.[12] Currently, UHMWPE-based materials are predominantly fabricated using subtractive methods such as turning or milling. In the context of additive manufacturing, the challenges posed by the high viscosity and poor fluidity of UHMWPE have been addressed by the blending of UHMWPE with other polymers such as polyethylene glycol or high-density polyethylene (HDPE). Ramli et al.[11] demonstrated that the incorporation of a 60% HDPE fraction improved the flowability and mechanical properties of UHMWPE for use in the FDM process. Additionally, Shokrgozar et al.'s research[13] confirmed the excellent biocompatibility of blended UHMWPE/HDPE composites *in vitro*.

However, the integration of such materials presents a significant engineering challenge due to their physical and chemical disparities.[14] Various techniques for combining dissimilar materials, particularly in polymer–metal hybrid structures, have emerged in recent years. Among these methods, "form fits" offer numerous advantages and significant potential for connections.[15] Wolf et al.[16,17,19] demonstrated that the incorporation of undercuts in joining structures can enhance adhesive joint strength through the introduction of mechanical interlocking, with the tensile adhesive strength of a 25°-undercut specimen surpassing those of specimens with other angles. Therefore, this method may be deemed appropriate for the development of an innovative TMJ prosthesis.

Currently, existing TMJ prostheses lack the incorporation of an articular disc and cartilage, which has significant biomechanical implications. As a result, there is a deficiency in physiological elasticity during the motion of TMJ prostheses, leading to an inability to fully meet the functional requirements of mandibular movement and potentially compromising long-term stability.

In the present study, we explored the use of biomimetic articular elastic layers composed of a UHMWPE/HDPE blend implemented in the condyle component to enhance the elasticity of TMJ prostheses. Ti–6Al–4V alloy was employed for biomimetic residual mandible prostheses, and UHMWPE was utilized for biomimetic articular elastic layers as a means to enhance the flexibility of TMJ condyle prostheses. The aim of this study was to establish hybrid structures comprising a UHMWPE/HDPE blend connected to a Ti alloy through form fits to replicate the interface between biomimetic articular elastic layers and the condyle component, and to assess their elasticity and adhesive strength.

2. Materials and methods

2.1. Materials and equipment

The UHMWPE used in this study was GUR 1020 (Ticona, Telford, UK) provided in powder form with a weight average molecular weight of 3.5×10^6 g/mol and a density of 0.93 g/cm^3. The HDPE used (PetroChina, Beijing, China) has a density of 0.954 g/m^3 and a weight average molecular weight of 1.2×10^5 g/mol. The material for the ramus of condyle prosthesis was Ti–6Al–4V alloy created using the Mlab Cusing 3D Metal Printing Machine (Concept Laser, Lichtenfels, Germany). The accuracy of the machine was approximately 40 μm.

UHMWPE with the addition of 60% HDPE was generated using a double-screw extruder. The resulting samples were formed into particles with an average diameter of 2 mm and subjected to preliminary print testing using a print-head nozzle with a diameter of 0.5 mm (Figure 1). We used our self-developed FDM 3D printer, which allows the manipulation of a large number of printing parameters: printing temperature (T), layer height (LH), printing speed (PS), printing acceleration (A), and flow rate (F).[18] After numerous printing runs, we determined the optimal printing parameters to be: T = 240°C, LH = 0.2 mm, PS = 350 mm/min, A = 0 mm/min^2, and F = 100%.

2.2. Design and mechanical testing of the articular elastic layer component

The porous model, designed using Simplify 3D software (Simplify3D, Ohio, America), featured a wire harness staggered structure aimed at reducing the material's elastic modulus to align with TMJ disc performance requirements. The porosity of the array was adjusted by manipulating parameters such as wire harness spacing and alternating angle. Specifically, wire harness spacings of 0.4, 1.0, and 1.6 mm were utilized. The alternating angle between the harnesses was set to 0°/30°, 0°/45°, 0°/60°, and 0°/90° (Figure 2). A standard 10 × 10 × 10 mm^3 cube structure was 3D-printed for each sample set to assess its compressive elastic modulus and maximum compressive strength using a universal testing machine (Figure 3). A total of six specimens were tested in each sample set.

2.3. Design and preparation of metal bone and elastic layers connection structure

First, the condyle component (Ti–6Al–4V alloy) was produced by selective laser melting. In this study, the condyle prosthesis was designed as a cube model (partner A) with geometrical dimensions of 30 × 10 × 10 mm^3 to facilitate the measurement of the joining strength. At the top of partner A, three rows with pin structures were located, consisting of three pins. In total, the joining

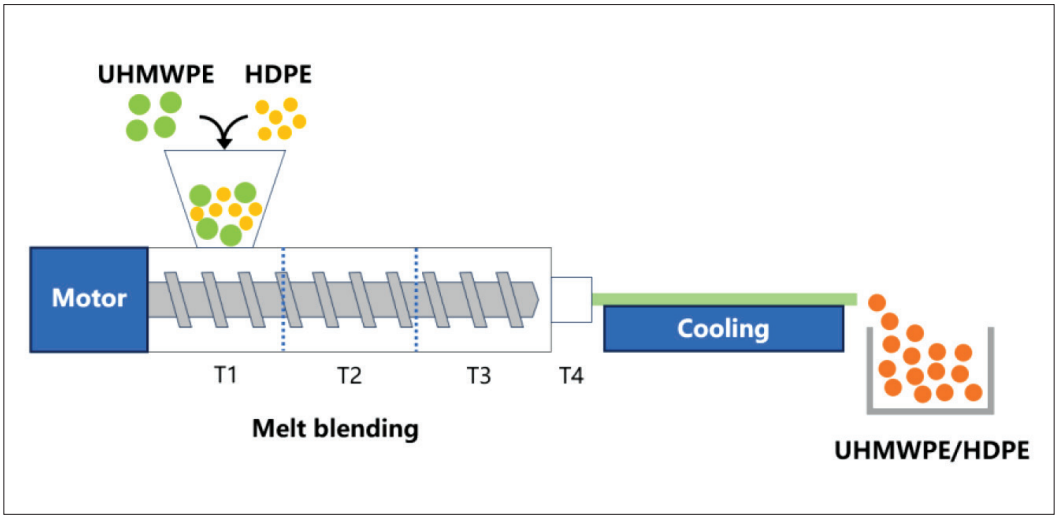

Figure 1. Preparation of UHMWPE with the addition of 60% HDPE using a double-screw extruder. Abbreviations: HDPE, high-density polyethylene; UHMWPE, ultra-high-molecular-weight polyethylene.

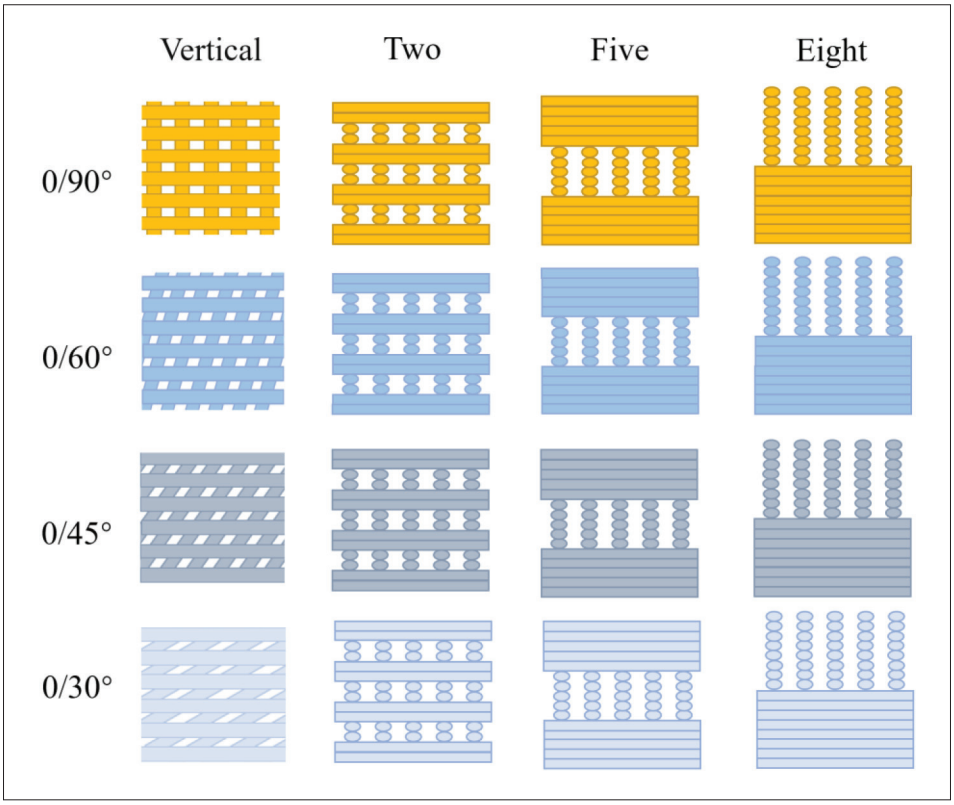

Figure 2. Schematics of porous scaffolds with distinct structural features having alternating angles of 0°/30°, 0°/45°, 0°/60°, and 0°/90°, and two, five, or eight crossing layers.

Figure 3. Universal testing machine.

surface had nine pins, which allowed for a doubled number of undercut structures (two undercut sections per pin). The section of the pin structure was trapezoid and defined by three parameters: the undercut angle, open width, and undercut depth. Their specific values are shown in Figure 4. We fabricated the undercut angle to 25° because this angle was found to significantly improve the tensile adhesive strength.[15] The material between the UHMWPE/HDPE condylar head and the titanium alloy riser was the UHMWPE/HDPE material.

Subsequently, a blend of UHMWPE with 60 wt% HDPE was utilized as the biomimetic material for articular elastic layers. This ratio has been determined to effectively enhance the processability of UHMWPE.[11] The composite material was heated to 180°C until it reached a molten state, and it was then extruded into the pin structure of the condyle component using a heated Al plate. It is crucial that the molten material completely covers the Ti alloys, serving as the base for the prepared biomimetic articular elastic layers. The scaffold structure of the printed elastic layer material is interconnected through welding with a welding plate temperature of 120°C. Biomimetic articular elastic layer specimens measuring 30 × 10 ×

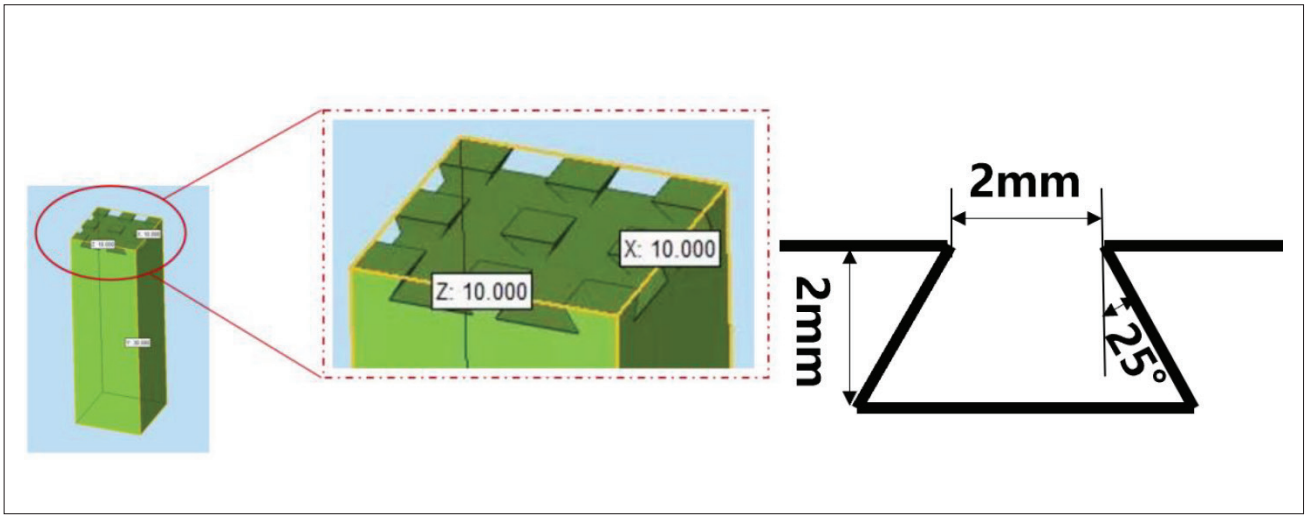

Figure 4. The joining surface. The joining surface with nine pin structures. The undercut angle was 25°. The open width and undercut depth were 2 mm.

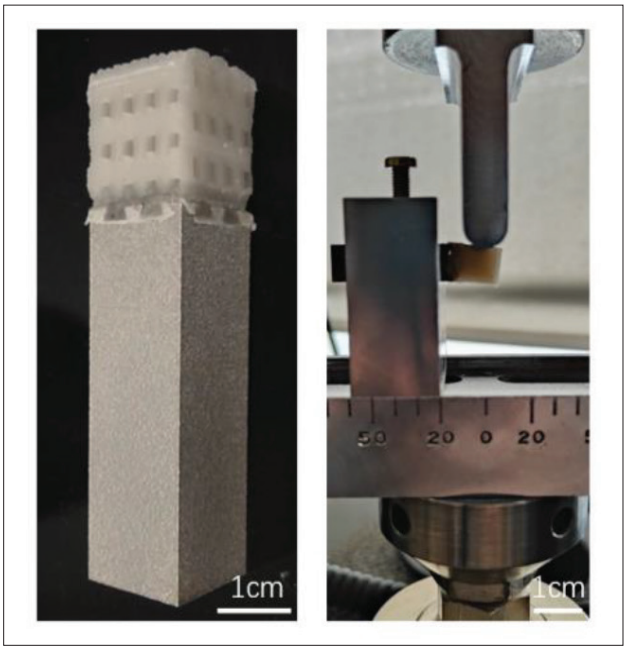

Figure 5. Shear strength measurements using the universal testing machine.

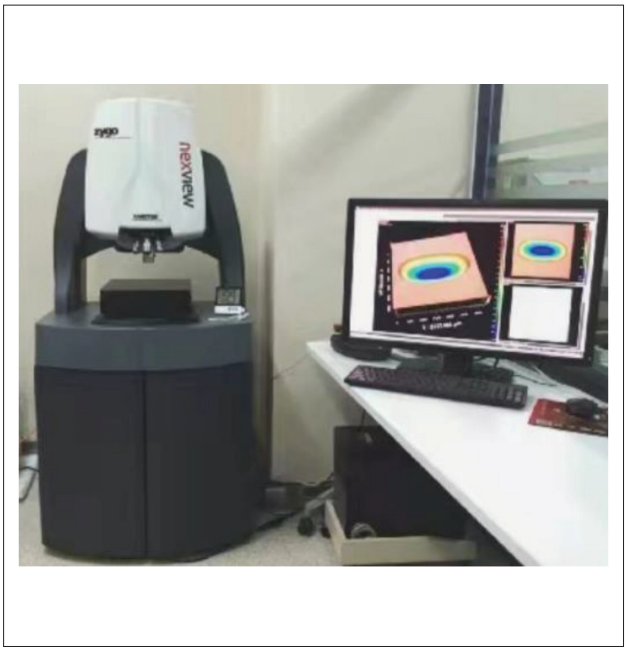

Figure 6. The white light interferometer used in this study.

10 mm^3 were produced using the FDM technique. The resulting specimen is depicted in Figure 5. Shear strength measurements were conducted using a universal testing machine equipped with a specialized membrane. The shear test was conducted using a specialized mold that applied vertical force on the superior material at 25°C, with a mold descending speed of 1 mm/min.

2.4. Polishing and surface-roughness measurement

The surface of the TMJ UHMWPE head must undergo polishing to mitigate the potential increase in wear degree and subsequent inflammatory response.[19] Ten samples resembling condylar heads were fabricated and subjected to polishing with sandpaper of varying mesh sizes (500, 800, 1000, 1200, and 1500). The average surface roughness

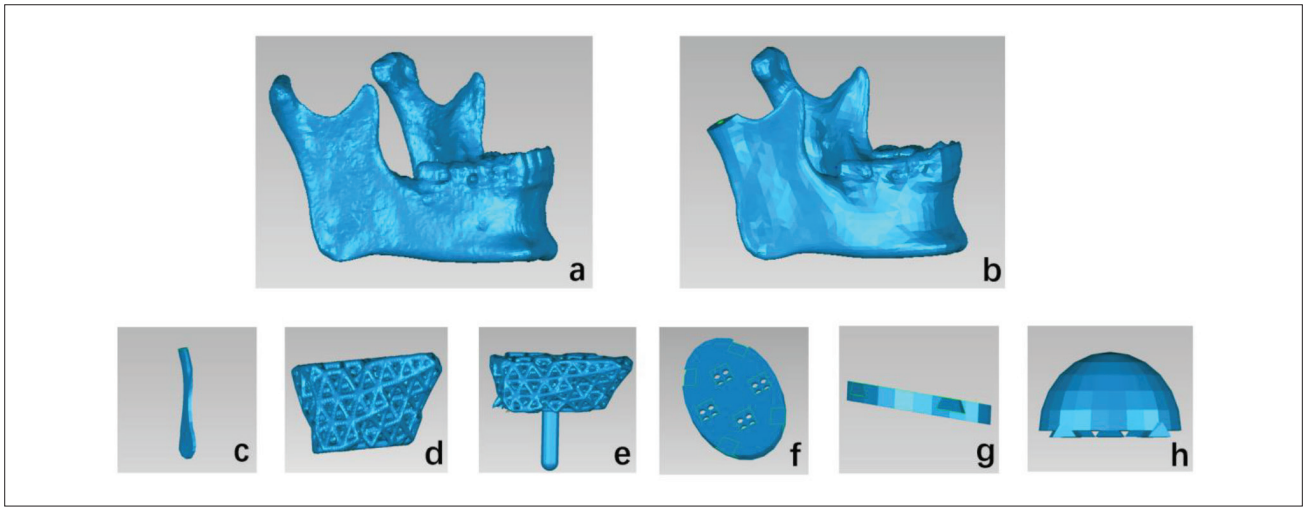

Figure 7. Design of the human condyle prosthesis**.** (a) 3D reconstruction of the subject's TMJ. (b) Simulated condylar defect. (c) Onlay plate. (d) Metal tetrahedral scaffolding structure. (e) Inlay rod. (f) Top view of the connecting structure. (g) Side view of the connection structure. (h) Bionic articular elastic layer structure. Abbreviation: TMJ, temporomandibular joint.

(Sa) of the joint head was measured with a white light interferometer (Figure 6). Three points were selected from the uppermost section of each sample to measure the surface roughness, and the average of these measurements was calculated to represent the roughness value.

2.5. Design and preparation of the human condyle prosthesis

We recruited one volunteer with healthy TMJ at the Department of Oral and Maxillofacial Surgery of Peking University School and Hospital of Stomatology, China (PKUSSIRB-201942015). Computed tomography (CT) images were acquired using 3D Accuitomo (Morita, Japan). Simulated arthrotomy was performed under the condylar neck. An 8-mm-high ellipsoidal bionic articular elastic layer was designed and the remaining space was filled with a metal tetrahedral scaffolding structure with a mean cell size of 2280 μm and a strut diameter of 570 μm. The primary significance of the porous structure lied in its ability to reduce the elastic modulus of the metal, which minimized stress shielding and reduced bone resorption around the prosthesis. This feature could promote muscle and bone integration, improving connectivity.[20] There were eight concave connection structures in the middle of the elastic layer and the metal with an additional concave connection structure positioned 2 mm apart. Sixteen 2 × 2 × 2 mm rejection holes were set above the metal to increase the connection strength. According to our previous research, a 1.5-mm-thick onlay

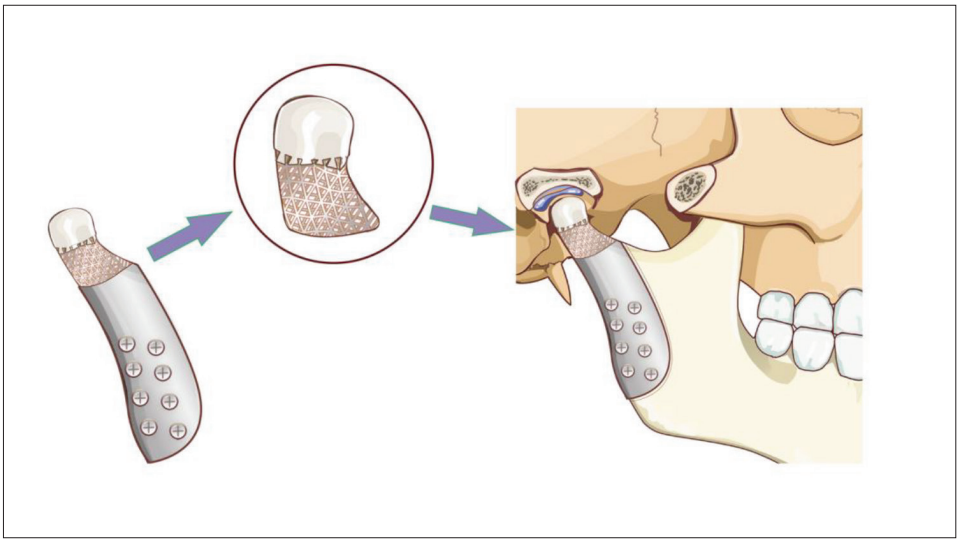

Figure 8. TMJ prosthesis design model. Abbreviation: TMJ, temporomandibular joint.

Figure 9. The head of the TMJ prosthesis. Abbreviation: TMJ, temporomandibular joint.

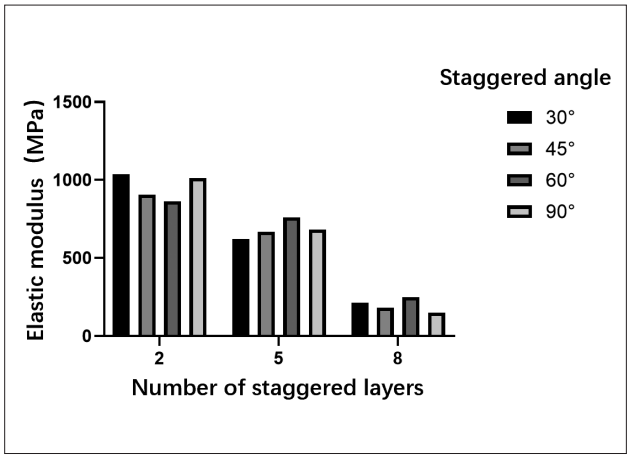

Figure 10. Elastic moduli of scaffold structures with varying staggered layers and angles.

plate was designed for the external side of the mandible, an inlay rod was designed for under the support structure, and transition smooth treatment was performed at the joint to enhance their connectivity with the bone (Figure 7).

The mandibular brancvh metal prosthesis was initially printed based on the design specifications, followed by printing of the bionic articular cartilage. Subsequently, the two components were interconnected through welding to finalize the preparation process (Figure 8).

2.6. Mechanical testing of the condyle prostheses *in vitro*

Due to the limitations of the universal testing machine, the onlay rod and inlay plate were removed for this part of the study to simulate the actual prosthetic head. A compression test was conducted for the 3D-printed condylar prostheses using the universal testing machine. A total of six physical models were used for the compression tests (Figure 9). The test temperature was 25°C, and the mold descending speed was 1 mm/min.

3. Results

3.1. Compressive elastic modulus and compressive strength of bionic articular elastic layer internal scaffold structure

Six samples were tested for each bracket structure type, and the average value was calculated for the final result. Figure 10 illustrates the elastic moduli of scaffold structures with varying staggered layers and angles. The findings suggest that an increase in the number of staggered layers results in a decrease in elastic modulus, while the elastic modulus is not influenced by the staggered angle. Liu et al.[21] reported that a 0°/90° cross-angle scaffold structure exhibits superior rigidity. Therefore, we finally decided upon a bracket structure with a staggered layer number of eight and a wiring harness interleaving angle of 90°. The elastic modulus of this structure was measured to be 127.5 ± 16.1 MPa with a maximum compressive strength of 8.0 ± 1.3 MPa shown in Figure 11.

3.2. Connection strength

A total of six samples were tested to assess the strength of the connection between UHMWPE and the metal joint, with shear strength calculated using the formula $p = 3F/2A$, where F is force, and A is cross-sectional area. The strength curves for the Ti-6Al-4V–UHMWPE connection are shown in Figure 12. The average strength is 2.62 ± 0.98 MPa.

3.3. Roughness

Ten polished samples were tested and the polished sample was shown in Figure 13. The surface roughnesses of the

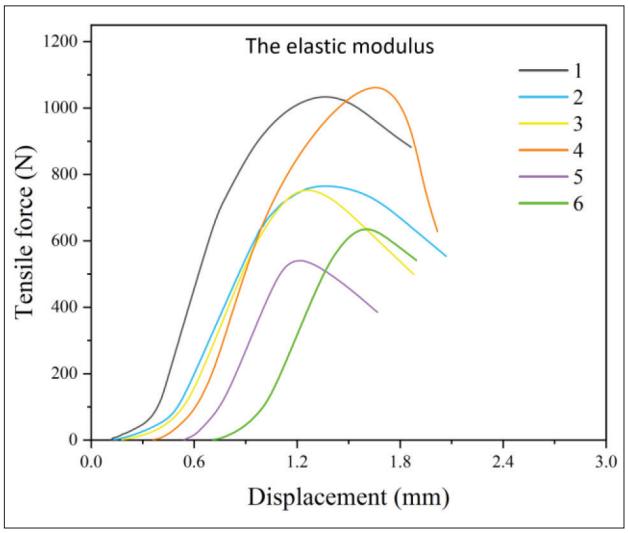

Figure 11. The elastic modulus of the structure with a staggered layer number of eight and a wiring harness interleaving angle of 90°.

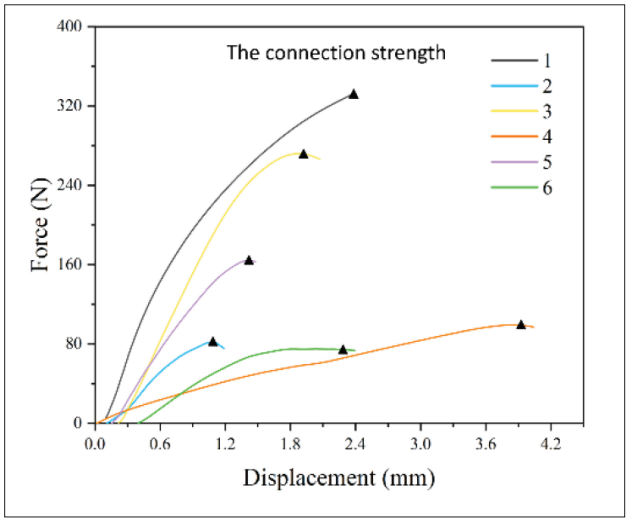

Figure 12. The connection strength of UHMWPE to the metal joint. Abbreviation: UHMWPE, ultra-high-molecular-weight polyethylene.

Figure 13. The polished samples. Comparison of polished and unpolished samples. The left sample was unpolished and the right one was polished.

condyle apexes after polishing were measured using a white light interferometer. Figure 14 shows the surface roughness after polishing (and after unfolding). The average roughness was 1.62 ± 0.13 μm.

3.4. Production and morphology analysis of TMJ prosthesis and elastic performance test of TMJ prosthesis

We effectively manufactured TMJ prostheses for healthy individuals in accordance with the procedures outlined in Section 2.5. Figure 15 shows the completed TMJ prostheses, which had already been polished. The elastic moduli of six prostheses were evaluated using a testing machine after removing the onlay plate and inlay rod. Figure 16 shows the elasticity modulus curves. An average modulus of 68 ± 0.32 MPa was recorded.

4. Discussion

The TMJ is the sole mobile joint in the oral and maxillofacial region and is the singular bilateral joint in the human body. It plays a crucial role in speech, mastication, deglutition, and other essential functions. TMJ tumors, joint ankylosis, trauma, and deformities can result in morphological abnormalities and functional impairment of the TMJ, impacting not only the esthetic aspect of patients' facial features but also causing physiological and psychological dysfunctions.[22] Artificial TMJ replacement is an effective approach for managing advanced stages of

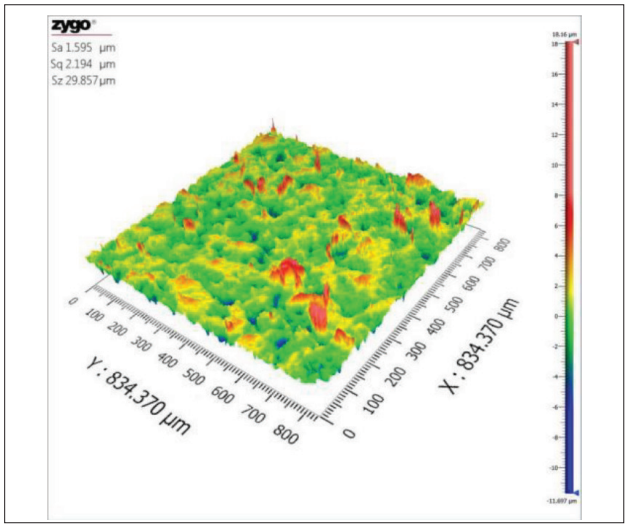

Figure 14. Surface roughness after polishing.

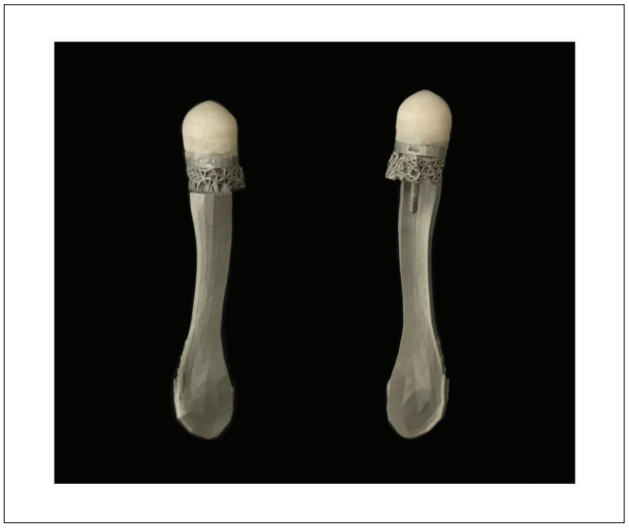

Figure 15. Completed TMJ prostheses.

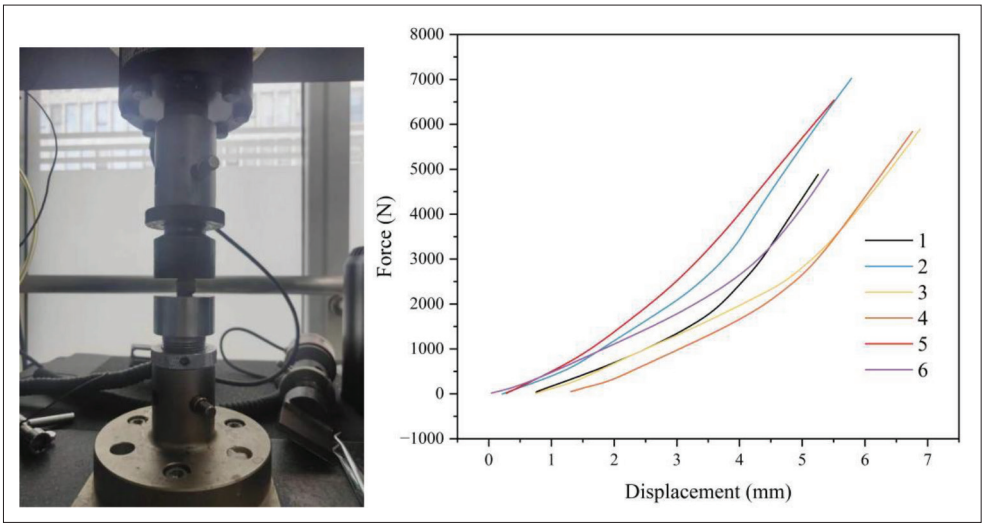

Figure 16. Compression experiment equipment and the resulting elasticity modulus curves.

TMJ disease.[23] Existing artificial joint prosthesis systems typically comprise a complete joint prosthesis consisting primarily of metal articular process prosthesis and a UHMWPE articular fossa prosthesis.[24] However, they lack the physiological elasticity of an actual articular disc, leading to constraints in functional movement and a barrier effect on stress distribution. Thus, the novel artificial joint prosthesis developed in this study utilized a hybrid UHMWPE/HDPE material for the bionic joint disc, resulting in an increased elasticity of the prosthesis. The elasticity of the new joint prosthesis was confirmed through mechanical testing.

The articular disc functions as a non-ossified structure within the TMJ, facilitating intricate movements and contributing significantly to jaw function by distributing stress, absorbing loads, and providing lubrication. The forces acting on the joint disc include compressive, tensile, and shear forces.[25] The articular disc is a kind of viscoelastic material. Barrientos et al.[6] reported that the behavior of the whole disc is primarily elastic, with some viscosity. Nickel et al.[6] demonstrated that the viscosity of a disc is augmented by a reduction in its elastic response, which is particularly evident under compressive loading conditions. Numerous investigations have evaluated the mechanical characteristics of joint discs from humans, sheep, and pigs, with their average compression modulus being a key parameter of interest. The average compression relaxation modulus and instantaneous compression modulus of a human joint disc at 20% strain are 37 and 1315 kPa, respectively.[26] Jiang et al.[27] analyzed the mechanical properties of 30 goat joint discs and found that the TMJ disc has certain compressive resistance (8.41 ± 2.12 MPa) and tensile resistance (9.54 ± 3.26 MPa). Yildirim et al.[28] used magnetic resonance imaging (MRI) to measure the elongation of the articular disc when the mouth is opened and closed, demonstrating its elastic properties. Hagandora et al.[29] reported that the elasticity of goat articular discs is better than that of the condylar cartilage. Many studies have demonstrated the importance of elasticity in joint discs, which is essential for the function of artificial joint prostheses.[6,27]

Currently, there are no materials that accurately replicate the properties of articular discs. Research in the field primarily centers on tissue engineering, material composition, and mechanical properties.[30–32] Some progress has recently been made in the field of 3D-printed scaffolds based on polycaprolactone (PCL) to simulate TMJ discs.[30] A novel synthetic TMJ disk was developed utilizing polyvinyl alcohol hydrogels and 3D-printed PCL, serving as an artificial joint disk reinforced through cyclic freeze-thawing crosslinking and PCL implantation.[31] Jiang et al.[32] developed a prosthesis construct with laser-drilled decellularized natural disc reinforced by PCL, which mimics the natural morphology, and structural, biomechanical, and biological property of the TMJ disc.

UHMWPE exhibits favorable properties such as wear resistance, impact resistance, self-lubricity, viscoelasticity, and corrosion resistance. The viscoelastic characteristics of UHMWPE are akin to those of the TMJ disc, which boasts exceptional compression and elastic properties.[25] In the field of orthopedics, 3D printing technology has found widespread application in the development of medical prostheses. This technology enables the modification of internal scaffold structures to lower a material's elastic modulus, allowing it to mimic the properties of human tissue.[6] UHMWPE is ill-suited to 3D printing due to its high viscosity and limited fluidity. In this study, HDPE was incorporated into UHMWPE using twin-screw blending

technology at a 6:4 ratio, and the resulting material was successfully utilized in FDM 3D printing, consistent with Ramli et al.'s study.[11] Thus, the challenge of 3D-printing UHMWPE was effectively addressed. The porous structures produced through 3D printing offer customizable pore size, shape, and porosity. The porous structure has the advantages of a low Young's modulus, high compressive strength, and abundant cell space for bone tissue engineering.[33] There is a stress barrier effect between the implant and the metal prosthesis, and the reduced stiffness of the implant will increase the shear stress between the implant and the surrounding bone.[34,35] There have been many attempts to make different metal scaffold structures with decreased elastic moduli that achieve the performance of bone. Wang et al.[36] produced Ti with a porosity of 32–47% that exhibited excellent Young's moduli in the range 23–62 GPa, and Barui et al.[37] designed a porous Ti-6Al-4V implant with an elastic modulus of 2.2–3.0 GPa. Li et al.[38] fabricated pure porous Ti with 50–70% porosity and different pore sizes by diffusion bonding. The Young's moduli of the materials were in the range of 1.0–7.5 GPa, and the yield stress was between 10 and 110 MPa. Thus, current developed materials have the Young's moduli of the GPa scale, presenting a notable disparity from that of the MPa scale of joint discs and articular cartilage, thereby posing challenges in achieving the desired elasticity for artificial joints.

This study utilized HDPE-modified UHMWPE and employed a rationally designed internal scaffold structure. The Young's modulus of 127.5 MPa obtained in this study aligns closely with the findings of Salimon et al.[39] regarding porous UHMWPE and the Young's moduli of the human joint discs. Additionally, the compressive strength of 8 MPa exceeds that of the human joint disc.[25] While maintaining adequate compressive strength, the prosthesis in this study had an elastic modulus that was significantly lower than that of current joint prostheses, including those with optimized internal pore structures.[40] This is a significant advancement. Currently, total joint replacement is complex and carries potential risks, including abnormal mandibular motor function and joint stiffness, which can impact movement in the healthy joint.[2,41] The enhanced flexibility of the joint head may allow for hemijoint replacement, a less invasive alternative that involves preserving the joint disc and only replacing the joint head, which is encompassed in a simpler operation with minimal impact on the healthy joint.

A variety of approaches have been recently proposed to join metals to polymers, including adhesive bonding, mechanical fasteners, joining processes, and direct assembly.[42] The study applied surface texture patterning to a Ti–6Al–4V alloy surface to better establish a connection with UHMWPE. A 25°-undercut-angle micropattern structure was utilized to achieve this connection, resulting in a shear strength of 2.62 MPa, which exceeds that experienced by articular discs.[43] This indicates that an integrated artificial Ti-6Al-4V–UHMWPE joint could meet the strength requirements of an artificial TMJ. Wear is the main factor in bone resorption and aseptic implant loosening of artificial TMJ replacement, contributing to long-term implant failure.[44,45] The rate of wear can be influenced by both material-related factors such as material choice, surface roughness, and factors related to the patient's jaw movement.[46] Even with the "gold-standard" biocompatibility of Co–Cr–Mo alloy and UHMWPE, wear debris can still appear.[2] In this research, the condyle head was modified to an elastic UHMWPE material to enhance the elasticity of the TMJ prosthesis and minimize wear, while the surface was polished to a roughness of 1.5 μm to better comply with artificial joint standards.[47] However, a wear test was not performed in this study as the prosthesis was customized, and there is currently no available equipment for customized TMJ fatigue testing. Based on the researches related to customized joint prostheses and movement of mandible, future studies could involve the development of a customized TMJ simulator to enable fatigue testing.

5. Conclusion

The current study has effectively implemented the design, fabrication, and modification of an artificial TMJ, whose elastic properties are superior to current joint prostheses. The new TMJ shows potential as a product for clinical application, introducing innovative concept of an elastic joint prosthesis, which could greatly enhance the performance of existing joint prostheses. Currently, only the elastic properties of the artificial TMJ have been evaluated. The overall elastic modulus was measured to be 68 MPa, indicating a slight reduction compared to simple biomimetic elastic layer material. Previous studies have established that the elastic modulus of two connected porous materials was influenced by the weakest segment.[48] This observed reduction in elastic modulus may be attributed to alterations in the shape structure. Since joint prosthesis implantation in animals was not performed in this study, we will carry out *in vivo* tests for further verification in subsequent studies.

Acknowledgments

None.

Funding

This work was supported by grants from Beijing Municipal Science & Technology Commission (Z201100005520055) and Clinical Research Foundation of Peking University School and Hospital of Stomatology (PKUSS-2023CRF205).

Conflict of interest

The authors declare they have no competing interests.

Author contributions

Conceptualization: Junqi Jiang, Xiangliang Xu, Chuanbin Guo
Formal analysis: Bingxue Cheng
Investigation: Junqi Jiang, Zhiwei Jiao, Jianmin Han, Bingxue Cheng
Methodology: Zhiwei Jiao, Jianmin Han
Writing – original draft: Junqi Jiang
Writing – review & editing: Xiangliang Xu, Chuanbin Guo

Ethics approval and consent to participate

The biomedical ethics committee of Peking University Hospital of Stomatology approved this study (PKUSSIRB-201942015). All procedures performed in studies involving human participants were in accordance with the ethical standards of the institutional and/or national research committee and with the 1964 Declaration of Helsinki and its later amendments or comparable ethical standards. Written informed consent was obtained from all participants.

Consent for publication

Informed consent was obtained from the participants for the publication of their data.

Availability of data

Data are available from the corresponding authors upon reasonable request.

References

1. Yoda T, Ogi N, Yoshitake H, et al. Clinical guidelines for total temporomandibular joint replacement. *Jpn Dent Sci Rev*. 2020,56(1):77-83. doi: 10.1016/j.jdsr.2020.03.001
2. Elledge R, Mercuri LG, Attard A, et al. Review of emerging temporomandibular joint total joint replacement systems. *Br J Oral Maxillofac Surg*. 2019,57(8):722-728. doi: 10.1016/j.bjoms.2019.08.009
3. De Meurechy N, Mommaerts MY. Alloplastic temporomandibular joint replacement systems: a systematic review of their history. *Int J Oral Maxillofac Surg*. 2018;47(6):743-754. doi: 10.1016/j.ijom.2018.01.014
4. Tanaka E, van Eijden T. Biomechanical behavior of the temporomandibular joint disc. *Crit Rev Oral Biol Med*. 2003;14(2):138-150. doi: 10.1177/154411130301400207
5. Jibiki M, Shimoda S, Nakagawa Y, et al. Calcifications of the disc of the temporomandibular joint. *J Oral Pathol Med*. 1999;28(9):413-419. doi: 10.1111/j.1600-0714
6. Barrientos E, Pelayo F, Tanaka E, et al. Dynamic and stress relaxation properties of the whole porcine temporomandibular joint disc under compression. *J Mech Behav Biomed Mater*. 2016;57:109-115. doi: 10.1016/j.jmbbm.2015.12.003
7. Xu X, Zhang J, Luo D, et al. Biomechanical comparison between the custom-made mandibular condyle prosthesis and total temporomandibular joint prosthesis in finite element analysis. *Acta Bioeng Biomech*. 2020;22(4):151-160. doi: 10.37190/ABB-01721-2020-03
8. Geetha M, Singh AK, Asokamani R, Gogia AK. Ti based biomaterials, the ultimate choice for orthopaedic implants-a review. *Prog Nat Sci Mater*. 2009;54(3):397-425. doi: 10.1016/j.pmatsci.2008.06.004
9. Kurtz S., ed. *UHMWPE Biomaterials Handbook–Ultra-high Molecular Weight Polyethylene in Total Joint Replacement and Medical Devices*, third ed. Amsterdam: Elsevier Inc.; 2016.
10. Ponader S, von Wilmowsky C, Widenmayer M, et al. In vivo performance of selective electron beam-melted Ti-6Al-4V structures. *J Biomed Mater Res A*. 2010;92:56-62. doi: 10.1002/jbm.a.32337
11. Ramli MS, Wahab MS, Ahmad M, and Bala AS. FDM preparation of bio-compatible UHMWPE polymer for artificial implant. *ARPN J Engd Appl Sci*. 2016;11(8). 5474-5480.
12. Musib MK. A review of the history and role of UHMWPE as a component in total joint replacements. *Int J Biol Sci*. 2012;1(1):6-10. doi: 10.5923/j.ijbe.20110101.02
13. Shokrgozar MA, Farokhi M, Rajaei F, etc. Biocompatibility evaluation of HDPE-UHMWPE reinforced β-TCP nanocomposites using highly purified human osteoblast cells. *J Biomed Mater Res A*. 2010;95(4):1074-1083. doi: 10.1002/jbm.a.32892
14. Amancio-Filho ST, Santos JFD. Joining of polymers and polymer-metal hybrid structures: recent developments and trends. *Polym Eng Sci*. 2009;49(8):1461-1476. doi: 10.1002/pen.21424
15. Wolf M, Kleffel T, Leisen C, Drummer D. Joining of incompatible polymer combinations by form fit using the vibration welding process. *Int J Polym Sci*. 2017; 2017:1-8. doi: 10.1155/2017/6809469
16. Wolf M, Hertle S, Drummer D. Influence of the thermomechanical properties on the joining of adhesion incompatible polymers by form-fit using the vibration welding process. eXPRESS Polym Lett. 2019,13(4):365-378. doi: 10.3144/expresspolymlett.2019.30

17. Matsuzaki R, Tsukamoto N, Taniguchi J. Mechanical interlocking by imprinting of undercut micropatterns for improving adhesive strength of polypropylene. *Int J Adhes Adhesiv*. 2016;68:124-132. doi: 10.1016/j.ijadhadh.2016.03.002

18. Barrios JM, Romero PE. Decision tree methods for predicting surface roughness in fused deposition modeling parts. *Materials (Basel)*. 2019;12(16):2574. doi: 10.3390/ma12162574

19. Jedenmalm A, Affatato S, Taddei P, et al. Effect of head surface roughness and sterilization on wear of UHMWPE acetabular cups. *J Biomed Mater Res A*. 2009;90(4):1032-1042. doi: 10.1002/jbm.a.32161

20. Xu X, Luo D, Guo C, Rong Q. A custom-made temporomandibular joint prosthesis for fabrication by selective laser melting: Finite element analysis. *Med Eng Phys*. 2017;46:1-11. doi: 10.1016/j.medengphy.2017.04.012

21. Liu H, Ahlinder A, Yassin MA, et al. Computational and experimental characterization of 3D-printed PCL structures toward the design of soft biological tissue scaffolds. *Mater Design*. 2020;188:11. doi: 10.1016/j.matdes.2020.108488

22. Vega LG, González-García R, Louis PJ. Reconstruction of acquired temporomandibular joint defects. *Oral Maxillofac Surg Clin North Am*. 2013;25(2):251-269. doi: 10.1016/j.coms.2013.02.008

23. Mercuri LG. Costochondral graft versus total alloplastic joint for temporomandibular joint reconstruction. *Oral Maxillofac Surg Clin North Am*. 2018;30(3):335-342. doi: 10.1016/j.coms.2018.05.003

24. Burgess M, Bowler M, Jones R, et al. Improved outcomes after alloplastic TMJ replacement: analysis of a multicenter study from Australia and New Zealand. *J Oral Maxil Surg*. 2014;72(7):1251-1257. doi: 10.1016/j.joms.2014.02.019

25. Stanković S, Vlajković S, Bošković M, et al. Morphological and biomechanical features of the temporomandibular joint disc: an overview of recent findings. *Arch Oral Biol*. 2013;58(10):1475-1482. doi: 10.1016/j.archoralbio.2013.06.014. Epub 2013 Jul 18. PMID: 23871384. doi: 10.1016/j.jmbbm.2015.12.003

26. Nickel JC, Iwasaki LR, Beatty MW, Marx DB. Laboratory stresses and tractional forces on the TMJ disc surface. *J Dent R*. 2004;83(8):650-654. doi: 10.1177/154405910408300813

27. Jiang N, Yang YT, Bi RY, et al. Comprehensive measurement and quantification of bio-mechanical properties of the temporomandibular joint disc. *Zhonghua Kou Qiang Yi Xue Za Zhi*. 2021;56(8):764-768. Chinese. doi: 10.3760/cma.j.cn112144-20210322-00133

28. Yildirim D, Dergin G, Tamam C, et al. Indirect measurement of the temporomandibular joint disc elasticity with magnetic resonance imaging. *Dentomaxillofac Radiol*. 2011;40(7):422-428. doi: 10.1259/dmfr/98030980

29. Hagandora CK, Chase TW, Almarza AJ. A comparison of the mechanical properties of the goat temporomandibular joint disc to the mandibular condylar cartilage in unconfined compression. *J Dent Biomech*. 2011;2011:212385. doi: 10.4061/2011/212385

30. Hu S, Yi Y, Ye C, et al. Advances in 3D printing techniques for cartilage regeneration of temporomandibular joint disc and mandibular condyle. *Int J Bioprint*. 2023;9(5):761. doi: 10.18063/ijb.761

31. Jiang N, Yang Y, Zhang L, et al. 3D-printed polycaprolactone reinforced hydrogel as an artificial TMJ disc. *J Dent Res*. 2021;100(8):839-846. doi: 10.1177/00220345211000629

32. Jiang N, Chen H, Zhang J, et al. Decellularized-disc based allograft and xenograft prosthesis for the long-term precise reconstruction of temporomandibular joint disc. *Acta Biomater*. 2023;159:173-187. doi: 10.1016/j.actbio.2023.01.042

33. Chen H, Han Q, Wang C, et al. Porous scaffold design for additive manufacturing in orthopedics: a review. *Front Bioeng Biotechnol*. 2020;8:609. doi: 10.3389/fbioe.2020.00609

34. Huiskes HWJ. Stress shielding and bone resorption in THA: clinical versus computer-simulation studies. *Acta Orthop Belg*. 1993; 59(Suppl 1):118-129.

35. Trebse R, Milosev I, Kovac S, et al. Poor results from the isoelastic total hip replacement. *Acta Orthop*. 2005;76(2): 169-176. doi: 10.1080/00016470510030535

36. Wang D, Li Q, Xu M, et al. A novel approach to fabrication of three-dimensional porous titanium with controllable structure. *Mater Sci Eng C Mater Biol Appl*. 2017;71:1046-1051. doi: 10.1016/j.msec.2016.11.119

37. Barui S, Chatterjee S, Mandal S, et al. Microstructure and compression properties of 3D powder printed T scaffolds with designed porosity: experimental and computational analysis. *Mater Sci Eng C Mater Biol Appl*. 2017;70(1):812-823. doi: 10.1016/j.msec.2016.09.040

38. Li F, Li J, Huang T, Kou H, Zhou L. Compression fatigue behavior and failure mechanism of porous titanium for biomedical applications. *J Mech Behav Biomed Mater*. 2017;65:814-823. doi: 10.1016/j.jmbbm.2016.09.035.

39. Salimon AI, Statnik ES, Zadorozhnyy MY, et al. Porous open-cell UHMWPE: experimental study of structure and mechanical properties. *Materials (Basel)*. 2019;12(13):2195. doi: 10.3390/ma12132195

40. Cheng KJ, Liu YF, Wang JH, et al. 3D-printed porous condylar prosthesis for temporomandibular joint replacement: design and biomechanical analysis. *Technol Health Care*. 2022;30(4):1017-1030.
doi: 10.3233/THC-213534

41. Bekcioglu B, Bulut E, Bas B. The effects of unilateral alloplastic temporomandibular joint replacement on the opposite-side natural joint: a finite-element analysis. *J Oral Maxillofac Surg*. 2017;75(11):2316-2322.
doi: 10.1016/j.joms.2017.05.017

42. Feistauer EE, Dos Santos JF, Amancio-Filho ST. A review on direct assembly of through-the-thickness reinforced metal-polymer composite hybrid structures. *Polym Eng Sci*. 2019;59(4):661-674.
doi: 10.1002/pen.25022

43. Lai W-FT, Bowley J, Burch JG. Evaluation of shear stress of the human temporomandibular joint disc. *J Orofac Pain*. 1998;12(2):153-159.
doi: 10.1016/S0278-2391(98)90138-0

44. Sagbas B, Durakbasa MN. Measurement of wear in orthopedic prosthesis. *Proc Int Cong Adv Appl Phys Mater Sci*. 2012;121(1):131-134.
doi: 10.12693/APhysPolA.121.131

45. Alonso A, Kaimal S, Look J, et al. A quantitative evaluation of inflammatory cells in human temporomandibular joint tissues from patients with and without implants. *J Oral Maxillofac Surg*. 2009; 67(4):788-796.
doi: 10.1016/j.joms.2008.09.010

46. Sinno H, Tahiri Y, Gilardino M, Bobyn D. Engineering alloplastic temporomandibular joint replacements. *McGill J Med*. 2010; 13(1):63.
doi: 10.26443/mjm.v13i1.252

47. De Meurechy N, Aktan MK, Boeckmans B, et al. Surface wear in a custom manufactured temporomandibular joint prosthesis. *J Biomed Mater Res B Appl Biomater*. 2022;110(6):1425-1438.
doi: 10.1002/jbm.b.35010

48. Bittner SM, Smith BT, Diaz-Gomez L, et al. Fabrication and mechanical characterization of 3D printed vertical uniform and gradient scaffolds for bone and osteochondral tissue engineering. *Acta Biomaterial.* 2019;90: 37-48.
doi: 10.1016/j.actbio.2019.03.041